C. R. Physique 3 (2002) 827–837

Physique appliquée/*Applied physics*

DOSSIER

DU COMBUSTIBLE NUCLÉAIRE AUX DÉCHETS : RECHERCHES ACTUELLES

FROM NUCLEAR FUELS TO WASTE: CURRENT RESEARCH

New conditionings for separated long-lived radionuclides

Christophe Guy [a]*, Fabienne Audubert [a], Jean-Eric Lartigue [a], Christelle Latrille [a], Thierry Advocat [b], Catherine Fillet [b]

[a] **CEA Cadarache, BP 108, 13108 St Paul-Lez-Durance, France**

[b] **CEA Marcoule, BP 171, 30207 Bagnols-sur-Céze, France**

Received 25 April 2002; accepted after revision 25 April 2002

Note presented by Édouard Brézin.

Abstract Long-lived radionuclides such as I^{129}, Cs^{135} and minor actinides can be incorporated in crystalline structures of several specific materials with high chemical durability. Apatites, zirconolite, monazites, thorium phosphate-diphosphate and hollandite are being studied at the CEA and among a scientific research group called NOMADE. A first step is devoted to the scientific feasibility dealing with elaboration and characterization of non-radioactive materials and studies of their chemical durability and radiation stability. Development of apatite for iodine and minor actinides, zirconolite for minor actinides, monazite for trivalent actinides and thorium phosphate–diphosphate for tetravalent actinides has reached the scientific feasibility. Cs conditioning in hollandite and phosphate minerals needs further studies. ***To cite this article: C. Guy et al., C. R. Physique 3 (2002) 827–837.***

high level waste / conditioning / ceramic matrices

Nouvelles matrices pour le conditionnement des radioéléments à vie longue

Résumé Les radioéléments à vie longue (Iode129, césium135 et actinides mineures) peuvent être incorporés dans des structures cristallines de matériaux spécifiques à haute durabilité chimique. Les apatites, la zirconolite, les monazites, le phosphate-diphosphate de thorium et la hollandite sont étudiés au CEA et dans le cadre d'un groupement de recherche (NOMADE). Une première étape est consacrée à la faisabilité scientifique visant à élaborer et caractériser les matériaux et à étudier leur durabilité chimique et leur comportement sous irradiation. Au stade actuel des recherches, le développement des apatites pour l'iode et les actinides, de la zirconolite, des monazites et du phosphate–diphosphate de thorium pour les actinides a atteint cette étape. Le conditionnement du césium dans la hollandite ou les minéraux phosphatés nécessite des développements supplémentaires. ***Pour citer cet article : C. Guy et al., C. R. Physique 3 (2002) 827–837.***

déchets de haute activité / conditionnement / céramiques matrices

* Correspondence and reprints.
E-mail address: christophe.guy@cea.fr (C. Guy).

S1631-0705(02)01377-4/REV

1. Introduction

The conditioning of long-lived radionuclides in new dedicated host phases is one aspect of the enhanced separation strategy in the framework of the 1991 French law. Research is conducted on the minor actinides (Am, Cm, Np) which constitute the main long-term radiotoxic inventory in high-level nuclear waste, and on some long-lived fission products (I^{129}, Cs^{135}, Tc^{99}) that are considered as environmentally 'mobile' [1].

The selection of matrices suitable for the durable conditioning of these radionuclides was oriented by bibliographic surveys on the development of specific matrices abroad, the radionuclide loading capacity of the mineral structure, the long-term containment performance (self-irradiation resistance and chemical durability given by natural analogues) and the fabrication process (melting or sintering). Different types of matrices have been developed depending on the radionuclide chemical nature (Table 1):

(1) *Apatite*, with the generic formula $M_{10}(XO_4)_6Y_2$(where $M = Ca^{2+}$, Pb^{2+}, Ba^{2+}, etc., $XO_4 = PO_4^{3-}$, VO_4^{3-}, SiO_4^{4-}, etc., and $Y = F^-$, Cl^-, OH^-, Br^-, I^-, etc.) is considered for conditioning iodine and actinides. Iodine is incorporated in the structure channel in a lead apatite $Pb_{10}(VO_4)_{6-x}(PO_4)_xI_2$. For tri and tetravalent actinides, a double substitution Ac(III,IV)/Ca(II) and PO_4/SiO_4 is needed for the electrical neutrality of the structures $Ca_{(10-x)}Ac(III)_x(PO_4)_{(6-x)}(SiO_4)_xF_2$ and $Ca_{(10-x)}Ac(IV)_x$-$(PO_4)_{(6-2x)}(SiO_4)_{2x}F_2$.

(2) *Zirconolite*, with the generic formula $Ca^{2+}Zr_x^{4+}Ti_{(3-x)}^{4+}O_7$ (where $0.8 < x < 1.35$), is suitable for accommodating the rare earth elements, hafnium, and the tri and tetravalent actinides by substitution at calcium and zirconium sites. Actinides (III) are incorporated in calcium site to give the following formula: $Ca_{(1-x)}Ac(III)_xZrTi_{(2-x)}Al_xO_7$; titanium is substituted by aluminium for charge balancing. Actinides (IV) are incorporated by substitution at zirconium sites: $CaAc(IV)_xZr_{(1-x)}Ti_2O_7$.

(3) *Monazite*, with the generic formula $LnPO_4$ can incorporated tri and tetravalent actinides: $Ln_{(1-x)}$-$Ac(III)_xPO_4$ solid solution for trivalent actinides and $Ln_{(1-2x)}Ca_xAc(IV)_xPO_4$ for tetravalent actinides.

(4) *Thorium phosphate–diphosphate*, $Th_4(PO_4)_4P_2O_7$ is suitable for tetravalent actinides by substitution at thorium site: $Th_{4-x}Ac(IV)_x(PO_4)_4P_2O_7$.

(5) *Hollandite* with the generic formula $A_2B_80_{16}$ (where A = mono or divalent element such as Ba^{2+}, B = Al, Ti, Fe) can be used for caesium conditioning by substitution at a barium site. Materials with the following formula are being studied: $BaCs_{0.28}(Fe_{0.82}Al_{1.46})Ti_{5.72}0_{16}$.

The development of these matrices are divided in two main steps:

(1) the scientific feasibility up to 2001–2002 includes the formulation and elaboration of non-radioactive materials by combining experimental physical and chemical characterization of the solid, and quantum chemistry calculations. Basic studies of leaching behaviour, such as the identification of mechanisms

Table 1. Different materials developed for separated long lived radionuclides conditioning. The scientific feasibility is reached when the materials are written in bold type

Radionuclides	Matrices	
Minors actinides	Britholites	$Ca_{10-x}Nd_x(PO_4)_{6-x}(SiO_4)_xF_2$
	Zirconolite	$(Ca_{1-x}Nd_x)ZrTi_{2-x}Al_xO_7$
	Monazites	$NdPO_4$
	Thorium phosphate–diphosphate	$Th_4(PO_4)_4P_2O_7$
Cs	Hollandite	$BaCs_{0,28}(Fe_{0,82}Al_{1,46})Ti_{5,72}O_{16}$
	Phosphate minerals	$CaCsNd(PO_4)_2$, $CsTh_2(PO_4)_3$
I	Apatite	$Pb_{10}(VO_4)_{4,8}(PO_4)_{1,2}I_2$

and aqueous alteration kinetics, are also being conducted. The scientific feasibility implies that the incorporation in the crystalline structure has been demonstrated by their surrogate (rare earth elements) for actinides and Tc^{99} and by stable isotope for I^{129} and $Cs^{135}$and that at least a 100-fold increase in chemical durability has been obtained compared to existing available ways of conditioning. Radiation stability is also studied, notably by external ion bombardments and using a natural analogue.

(2) The technical feasibility up to 2006 will focus on the actinides incorporation in the mineral structure, to validate the elaboration process. The long term behaviour will be also characterised: chemical durability taking into account geochemical conditions in disposal and radiation stability, including auto-irradiation experiments conducted with Pu^{238} or Cm^{244} incorporated in the mineral structure to study the effect of α decay. The elaboration feasibility at an industrial scale is also a crucial element for the technical feasibility. Furthermore, matrices flexibility to incorporate minor elements accompanying the separated elements due to processes performance, as well as to incorporate the daughters of radionuclides must be studied.

In the present paper, we focus on two examples in order to explain the scientific approach and to illustrate the main results obtained in formulation, ceramic elaboration, aqueous alteration kinetics and radiation stability: apatite for iodine and zirconolite, apatite for minor actinides.

2. Iodine immobilisation in apatite

2.1. Synthesis route

The formulation options are determined by the size of the iodide ion I^-, which has a considerably larger ionic radius than the anions generally found in apatites (F^-, Cl^-, etc.). It can thus be incorporated in a lead apatite: $Pb_{10}(VO_4)_{4.8}(PO_4)_{1.2}I_2$ [2,3]. The apatite ceramic is obtained by reactive sintering under pressure (25 MPa) at 700 °C of a lead iodide (PbI_2) pellet surrounded with a lead orthovanadophosphate $Pb_3(VO_4)_{1.6}(PO_4)_{0.4}$ according to the following reaction:

$$PbI_2 + 3Pb_3(VO_4)_{1.6}(PO_4)_{0.4} \leftrightarrow Pb_{10}(VO_4)_{4.8}(PO_4)_{1.2}I_2.$$

$Pb_3(VO_4)_{1.6}(PO_4)_{0.4}$ is not only a reactant for the final synthesis of $Pb_{10}(VO_4)_{4.8}(PO_4)_{1.2}I_2$, but also ensures iodine containment during the synthesis. The final product is a pellet containing a heart of $Pb_{10}(VO_4)_{4.8}(PO_4)_{1.2}I_2$ surrounded by the sintered lead orthovanadophosphate (Fig. 1). Microprobe analysis showed that iodine diffusion within the encapsulating ceramic did not exceed 400 µm, confirming that the iodine was totally immobilised during the fabrication process.

2.2. Influence of the PO_4/VO_4 ratio on the sintering temperature

Complementary studies were conducted on the $Pb_3(VO_4)_{(2-x)}(PO_4)_x$ solid solution, which is the reactant precursor, to evaluate the influence of the phosphate concentration on the sintering behaviour. The results of the isothermal sintering study showed that compositions with low phosphorus content (small x value) can be densified rapidly with a limited increase in grain size at 650 °C [4,5]. The next objective was to apply these results to a study of reactive sintering to synthesise iodoapatite. Sintering studies under load (25 MPa) were limited to two compositions, where $x = 0.2$ and $x = 0.4$. Expansion measurements showed that densification was obtained at temperatures above 540 °C for $x = 0.2$ and 580 °C for $x = 0.4$, i.e., at temperatures 160 and 120 °C below the initial reference value (700 °C, see Section 2.1). The relative density of the resulting ceramics exceeded 96%. SEM observations as well as XRD and microprobe analysis revealed no minor phases, and showed that the synthetic ceramic totally incorporated the iodine (within 5% of the calculated theoretical concentration).

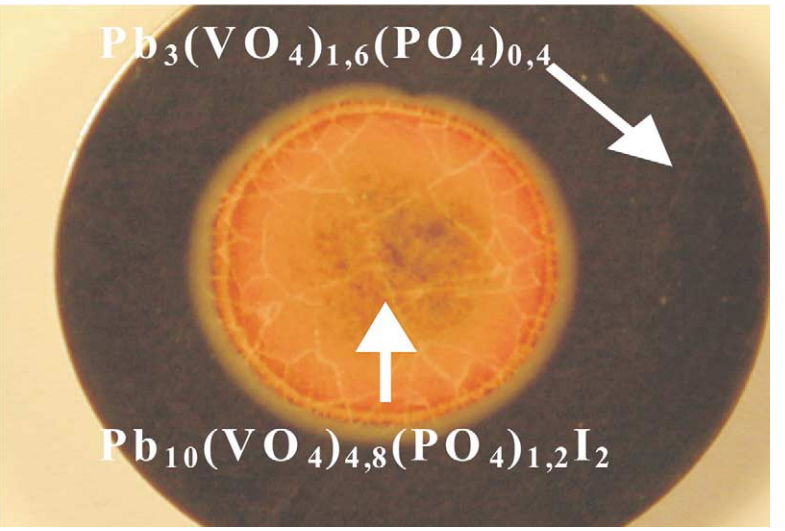

Figure 1. Pellet of 'iodine ceramic' sintered at 700 °C under 25 MPa (25 mm in diameter). At the centre, $Pb_{10}(VO_4)_{6-x}(PO_4)_xI_2$ appears in yellow surrounded by a lead orthovanadophosphate.

2.3. Chemical durability of iodoapatite

The initial leaching studies were carried out with powder and ceramic specimens of iodoapatite $Pb_{10}(VO_4)_{4.8}(PO_4)_{1.2}I_2$. Under standard alteration conditions (in pure water at 90 °C), iodine was released at an initial rate of $2.4 \times (\pm 0.3) \times 10^{-3}$ $g_{ceramic} \cdot m^{-2} \cdot d^{-1}$. Based on tests performed in pure water at 25, 50 and 90 °C, the apparent activation energy E_a of the dissolution reaction is about 37 ± 4 $kJ \cdot mol^{-1}$, corresponding to a rate increase by a factor of 1.5 every 10 °C. The effect of the pH on the dissolution rate was also investigated: the kinetics increase by an order of magnitude per pH unit in the range from pH 6 to pH 2. In alkaline media, the effect is less marked (Fig. 2).

The measurements of the concentration of the other constituents (Pb, V and P) showed that dissolution was not congruent. Characterisation studies on the altered solids using transmission electron microscopy (TEM) and X-ray photoelectron spectroscopy (XPS) show that Pb and V concentrations are controlled by the appearance of lead vanadates $Pb_2V_{1.16}P_{0.27}O_{7.66}$ (Fig. 3).

The initial dissolution rate decreases as a function of time (Fig. 4). Iodine diffusion through the layer induced by the dissolution selectivity or the secondary phases is suspected to be the controlling process for the long term iodine leaching.

3. Actinide conditioning

3.1. Actinide conditioning in britholite: Synthesis route

The formulation options were determined on the basis of studies of natural analogues. The apatitic structure seems capable of annealing the defects created by self-irradiation, even at low temperatures [6,7]. Studies of mineral phases crystallised during the natural nuclear reactions at Oklo showed that metamictisation (disruption of the crystal lattice) due to radiation damage (fission reactions, alpha particles and recoil nuclei) did not affect silicate apatites (britholites) with one silicate group and two fluorine atoms per cell. In Table 2, britholites sampled at In Ouzzal site (Algeria) exhibit different behaviour depending on their chemical composition. High phosphate content apatite remain crystallised even after irradiation dose up to 2×10^{19} α/g. On the other hand, high silica content apatite are found to be amorphous.

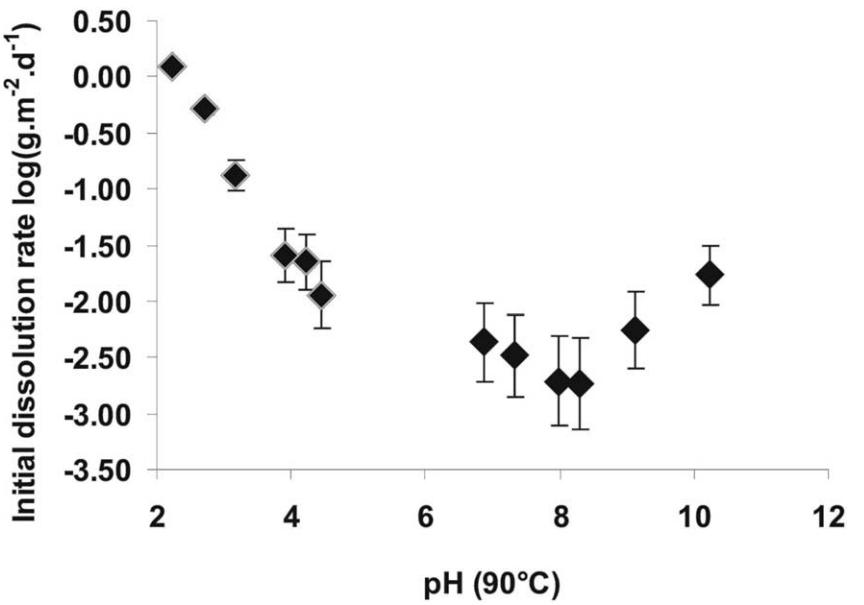

Figure 2. Initial dissolution rates of iodoapatite (powders and pellets) in water as a function of pH at 90 °C. Three different regions appear: (1) in acidic condition, the initial dissolution rate increases when pH decreases; (2) between pH 5 and 8, the dissolution rate is quite constant; and (3) in basic pH region, the dissolution rate increases with pH.

Figure 3. A lead vanado-phosphate is observed at the solid/solution interface (STEM) during the interaction between water and iodoapatite, confirming the preferential release of iodine in solution.

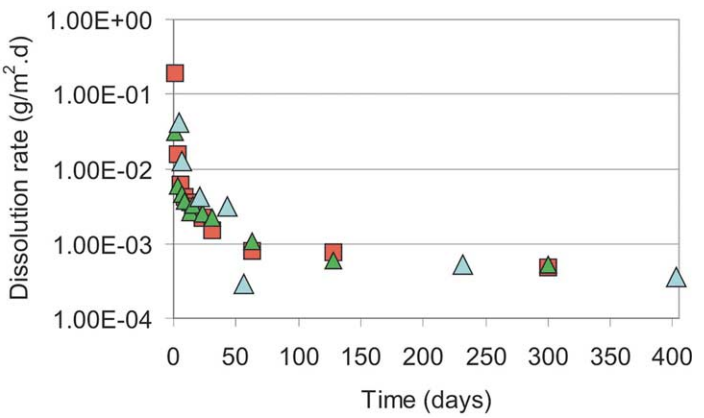

Figure 4. Evolution of the dissolution rate as a function of time. A decrease of the rate is observed as a function of time. A diffusion process is suspected to control the dissolution rate of iodine through secondary products (lead vanado-phosphate, see Fig. 3) or leached layer resulting from the preferential release of iodine in solution (red square: $S/V = 30\ \mathrm{cm}^{-1}$, green triangle: $S/V = 32\ \mathrm{cm}^{-1}$, blue triangle: $S/V = 80\ \mathrm{cm}^{-1}$; S material surface area, V water volume).

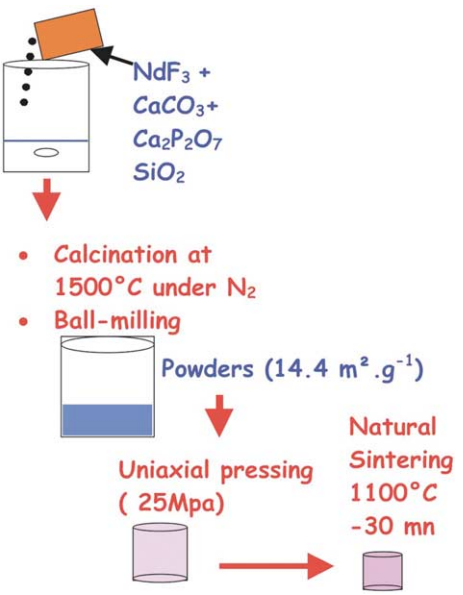

Figure 5. Britholite ceramic process for the actinide conditioning according to the following reaction: $NdF_3 + 5/2\,Ca_2P_2O_7 + SiO_2 + 9/2\,CaCO_3 \rightarrow Ca_9Nd(PO_4)_5(SiO_4)F_2 + 1/2\,CaF_2 + 9/2\,CO_2$.

For this reason, the mono-silicated britholite with the formula $Ca_9Nd(PO_4)_5(SiO_4)F_2$ (in which Nd simulates the trivalent actinides) was chosen for actinides conditioning. This structure is obtained by solid/solid reaction at 1500 °C and natural sintering at 1100 °C (Fig. 5; [8–10]).

3.2. Radiation stability of synthetic britholites

The radiation stability of britholites was investigated by external bombardment with lead and helium ions (simulating the recoil nuclei and the α particles respectively) and by in situ observation of changes in the material crystallinity [11]. An ion implanter coupled with a transmission electron microscope (Nuclear Spectrometry and Mass Spectrometry Center at Orsay, France) was used. The lifetime of the defects, which are created by the recoil nuclei and annealed (in the case of britholite) by the α particles, was measured as a function of the phosphate/silicate substitution ratio. This last parameter directly controls the Nd mass fraction in the material. The results showed that the effectiveness of the α annealing process was inversely proportional to the substitution ratio [11–14], as previously shown by the natural analogues. Together with

Table 2. Britholites from In Ouzzal site (Algeria). These data show the different behaviour toward α decay as a function of chemical composition

Samples	Ca	Si	P	F	U ppm	Th ppm	Dose α/g	State
INH604	8.9	0.67	5.28	1.54	315	6000	1.16×10^{19}	crystallised
INH187	8.29	1.12	4.82	1.60	150	9000	1.48×10^{19}	crystallised
INH604	7.70	1.76	4.15	1.56	350	14 000	2.40×10^{19}	crystallised
INH604	6.20	3.44	2.70	1.22	300	18 000	2.97×10^{19}	amorphous
INH603	4.56	5.41	0.64	1.06	280	9000	1.59×10^{19}	amorphous
INH603	4.15	5.76	0.69	1.30	350	14 000	2.40×10^{19}	amorphous

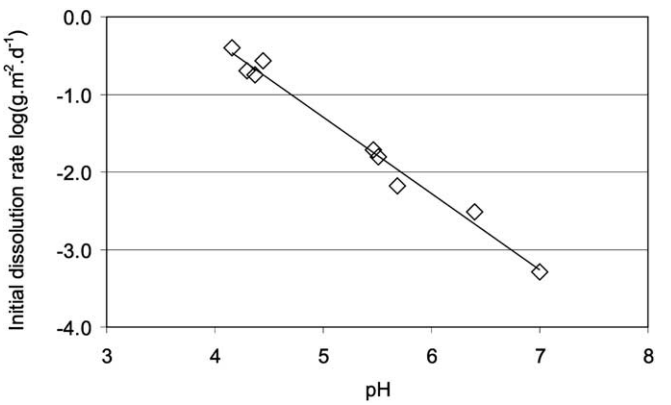

Figure 6. Initial alteration rate $r_{(0)}$ ($g{\cdot}m^{-2}{\cdot}d^{-1}$) of britholite (powders and pellets) as a function of pH.

the disorder creation data published in the literature, these results could now be used to assess the evolution of the disordered britholite fraction versus time, temperature and actinide concentration.

3.3. Chemical durability of britholite

The initial dissolution rates of britholite pellets were measured in initially pure water, at temperatures ranging from 25 to 100 °C, over short periods of time not exceeding 36 days. The key results are the following:

- the release of the most labile elements (as F^-, Ca^{2+}) indicate an incongruent dissolution mechanism during the first stages of the alteration process;
- the initial dissolution rates based on Ca release rate, is about 10^{-2} $g{\cdot}m^{-2}{\cdot}d^{-1}$ at 90 °C pH 5.7;
- a linear dependence was quantified at 90 °C between the initial dissolution rate $r_{(0)}$ and the pH of the leachate (Fig. 6), under slightly acid conditions and near neutral pH;
- a secondary phases (neodyme phosphate) is observed at the solid/solution interface.

Leach tests were conducted at 90 °C and under static conditions with large S/V ratios (S material surface area, V water volume) to evaluate the potential long-term dissolution rate. A steady state of Ca concentration is observed, suggesting a great decrease of the dissolution rate due to (i) thermodynamic equilibrium or (ii) solid/solution interface passivation due to secondary phases. New experiments under dynamic conditions are needed to identify the controlling process or processes.

3.4. Actinide immobilisation in zirconolite: Synthesis routes

Zirconolite $CaZr_xTi_{2-x}O_7$ ($0.8 < x < 1.37$) is one of a group of polytypic minerals capable of confining the rare earth elements (Nd, Ce, La, Gd), Hf and the actinides (U, Np, Am, Cm, Pu) by insertion at the calcium site for trivalent elements or the zirconium site for tetravalent elements site to give the following materials: $Ca_{(1-x)}Ac(III)_xZrTi_{(2-x)}Al_xO_7$ and $CaAc(IV)_xZr_{(1-x)}Ti_2O_7$.

They may be fabricated in three various ways:

- a ceramic process was developed in the late 1980s at ANSTO [15] in which Zr and Ti alkoxides are mixed with nitric acid solutions of Ca, Ln and/or actinides. The mixture is dried, calcined at about 700 °C, hot-pressed and sintered several hours at about 1400 °C (Fig. 7). This process was recently optimised [16], and leads to a single-phase Ln-doped ceramic, where $ZrTiO_4$ is the only minor phase ($\leqslant 0.5\%$), which does not contain actinide surrogates (Fig. 8(a));

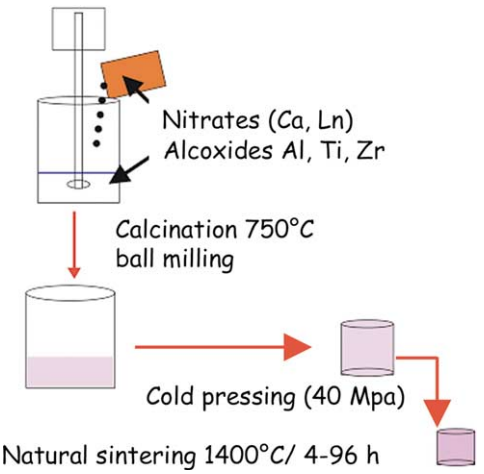

Figure 7. Ceramic process to prepare pure zirconolite ceramics. The synthesis route chosen to produce nearly pure zirconolite follows few steps. Firstly, a homogeneous amorphous precursor powder is made by hydrolysing a mixture of Al, Zr and Ti alkoxides with Ca and Nd nitrate solutions and excess water. After hydrolysis, the powder obtained is dried in an oven at 120 °C, then calcined at 750 °C for two hours and then milled using zirconia balls with water in order to get a very fine powder, which is dried again at 120 °C. This homogeneous amorphous powder is then pressed uniaxially under 40 MPa to form cylinders which are then sintered at 1400 °C for 96 h in an air atmosphere.

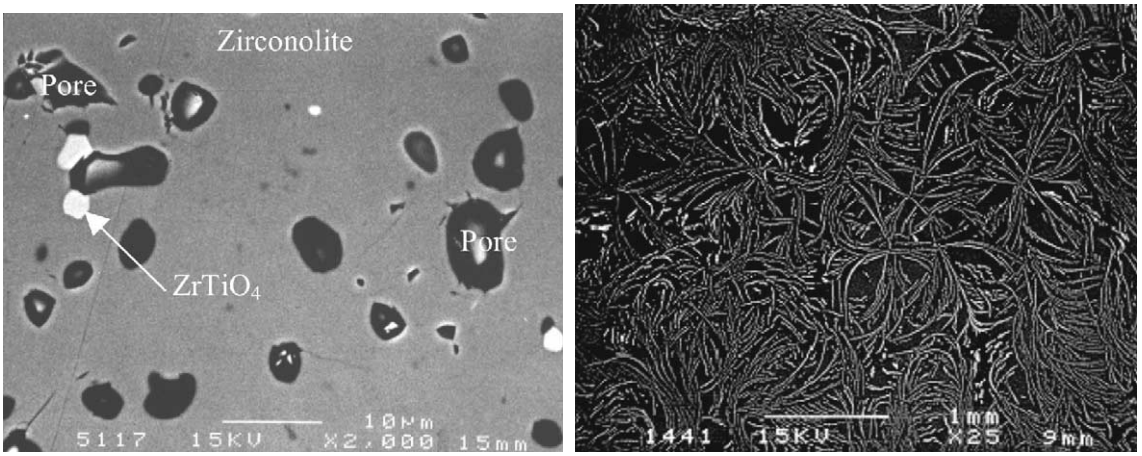

(a) (b)

Figure 8. (a) Backscattered electron (BSE) images of a sintered zirconolite ceramic (magnitude X2000); (b): BSE image of zirconolite glass–ceramic (magnitude X25): zirconolite needles are in light grey, the residual glass is dark grey.

- another process involves high-temperature melting of oxide mixtures at 1450–1800 °C for several hours, usually in a cold crucible melter, followed by controlled cooling to obtain zirconolite in glass–ceramic or ceramic form [17–22]. The melting process resulted in the formation of two types of zirconolite-enriched materials, according to the compositions of the oxide mixtures:
  - zirconolite glass–ceramics were fabricated by melting oxide mixtures at 1450 °C for one to two hours, pouring the material into an alumina crucible for heat treatment between 1050 to 1200 °C for up to 12 hours (devitrification of the parent glass), then furnace cooling to ambient temperature [17,19]. The silica-enriched residual glass represented about 60–70 vol% of the total (Fig. 8(b)); the actinide surrogates (Nd, Ce) were equally distributed between the residual glass and the zirconolite crystals;
  - zirconolite ceramics were fabricated by melting oxide mixtures at 1700–1800 °C for one to two hour, followed by a rapid quenching, which rate influences the final microstructure (grain size) of the ceramic [18,21]. The final ceramic contains mainly zirconolite (up to 70 vol%) with secondary phases such as zirconia, rutile, and perovskite which also incorporates Ln.

3.5. Chemical durability of zirconolite ceramics and glass ceramics

Aqueous alteration tests provided the following results (Fig. 9):

- the initial dissolution rates $r_{(0)}$ based on Ca release were determined in deionized water at temperatures ranging from 25 °C to 150 °C. Regardless of the test temperature, the initial zirconolite ceramic alteration rate was at least two orders of magnitude lower than the rate measured for the most resistant borosilicate and aluminosilicate glasses, and also zirconolite glass ceramics: approximately 10^{-2} g·m^{-2}·d^{-1} at 90 °C, for example;
- alteration at the initial rate $r_{(0)}$ was a transient phenomenon; the alteration rate for zirconolite ceramics quickly (within a few hours to a few days) diminished by several orders of magnitude to values below the determination limit, which is assumed to correspond to an absence of alteration. Similar trend was observed for zirconolite glass–ceramics, but the final rates $r_{(t)}$ are about one order of magnitude higher;

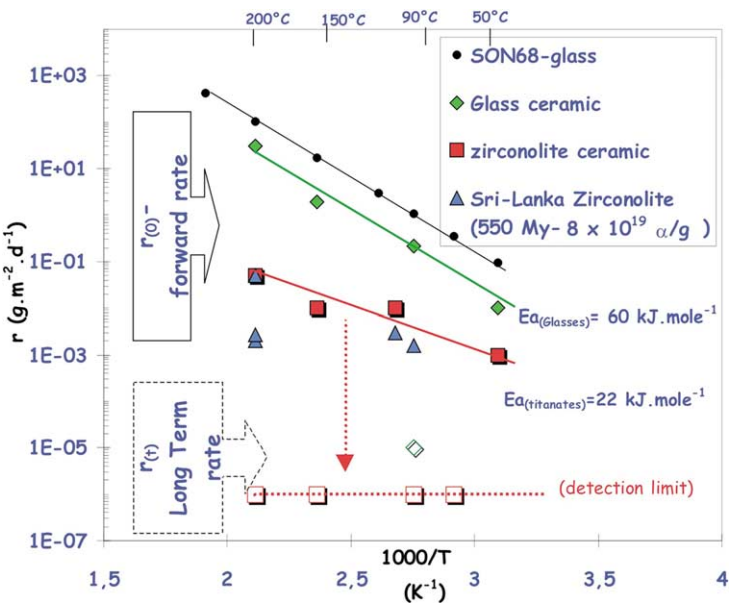

Figure 9. Dissolution rates for different materials (full symbols: $r_{(0)}$ initial dissolution rate; empty symbols: $r_{(t)}$ long term rates): SON68-glass which corresponds to the French nuclear glass, glass ceramic and zirconolite ceramic described in the text and a natural zirconolite mineral sampled in Sri-Lanka.

- thermodynamic calculations [16] have clearly indicated that the leachates were undersaturated with respect to the primary zirconolite phase, but saturated with respect to Ti, Zr and Al hydroxides, and oversaturated with respect to a decalcified zirconolite ($ZrTi_2O_6$) phase, which could act as a passivation layer;
- at temperatures below 100 °C, the pH (between 2 and 13) had little effect on the initial alteration rate: $r_{(0)}$ varied by less than an order of magnitude [23];
- published leached data of fully metamict (550 Million years old) naturally Th-enriched zirconolite (up to 20 wt% ThO_2), were reported on the arrhenius diagram (Fig. 9, [24]). The initial dissolution rate $r_{(0)}$ are similar to the values obtained with the synthetic fully crystalline zirconolite. These data suggest that even after structural transformation by an α-recoil nucleus, the chemical durability will not be fundamentally modified. More systematic data are still needed to be definitive on that point, notably by conducting leach tests with external heavy-ion irradiated ceramics [25,26] and, last but not least, with α-doped synthetic zirconolite ceramics.

4. Conclusions

Candidate matrices were selected after development studies on containment materials for long-lived radionuclides such as fission products (I, Cs) and minor actinides (Np, Am, Cm); material formulations and fabrication processes were developed at non-radioactive laboratory scale.

Lead orthovanadophosphate compounds such as $Pb_{10}(VO_4)_{4.8}(PO_4)_{1.2}I_2$ can incorporate up to 7 wt% iodine in the structure, with a good chemical durability.

REEs-doped Britholite such as $Ca_9Nd(PO_4)_6SiO_4F_2$ and REEs-doped zirconolite ceramics such as $Ca_{0.8}Nd_{0.2}ZrTi_{1.8}Al_{0.2}0_7$ can both confine up to 10 wt% oxide of trivalent and/or tetravalent actinide surrogates in their crystalline structures, with the requested enhanced chemical durability. The zirconolite glass–ceramic represents a compromise between the higher chemical durability of crystalline materials and the processing flexibility of glass.

After this first step, technical feasibility, up to 2006, needs to be demonstrated based on actinide incorporation in radioactive media, long term behaviour in term of chemical durability, radiation stability and elaboration at a representative scale toward an industrial application.

References

[1] T. Advocat, C. Fillet, F. Bart, G. Leturcq, F. Audubert, J.E. Lartigues, M. Bertolus, L. Campayo, C. Guy, in: Proceedings of the GLOBAL '01, International Conference on Back–End of the Fuel Cycle: From Research to Solutions, 9–13 September, 2001.
[2] F. Audubert, J. Carpéna, J.L. Lacout, F. Tétard, Solid State Ionics 95 (1997) 113–119.
[3] F. Audubert, J.-M. Savariault, J.-L. Lacout, Acta Crystallogr. C 55 (1999) 271–273.
[4] T. Robin, D. Bernache-Assollant, F. Audubert, J. Eur. Ceram. Soc. 20 (2000) 1231–1240.
[5] T. Robin, D. Bernache-Assollant, F. Audubert, Powder Technol. 103 (1999) 10–18.
[6] J. Carpena, in: P. Van den Haute, F. de Corte (Eds.), Advances in Fission Track Geochronology, Kluwer Academic, Dordrecht, 1998, pp. 81–92.
[7] J. Carpena, in: P. Van den Haute, F. de Corte (Eds.), Advances in Fission Track Geochronology, Kluwer Academic, Dordrecht, 1998, pp. 81–92.
[8] L. Boyer, Thèse, INP Toulouse, 1998.
[9] L. Boyer, J.-M. Savariault, J. Carpena, J.-L. Lacout, Acta Crystallogr. C 54 (1998) 1057–1059.
[10] L. Boyer, B. Piriou, J. Carpena, J.-L. Lacout, J. Alloys Compd. 311 (2000) 143–152.
[11] S. Soulet, J. Chaumont, J.C. Krupa, J. Carpena, J. Nucl. Mater. 289 (2001) 194–198.
[12] S. Ouchani, J.-C. Dran, J. Chaumont, Nucl. Intrum. Methods Phys. Res. B 132 (1998) 447–451.
[13] S. Soulet, J. Chaumont, J.C. Krupa, J. Carpena, Radiat. Eff. Defects Solids 155 (2001) 189–194.
[14] S. Soulet, J. Carpena, J. Chaumont, J.C. Krupa, M.O. Ruault, J. Nucl. Mater. 299 (2001) 227–234.
[15] E.R. Vance, C.J. Ball, M.G. Blackford, D.J. Cassidy, K.L. Smith, J. Nucl. Mater. 175 (1990) 58.
[16] G. Leturcq, P.J. Mcglinn, K.P. Hart, T. Advocat, C. Barbe, G.R. Lumpkin, in: Scientific Basis for Nuclear Waste Management, XXIV Mater. Res. Soc. Symp. Proc., Sydney, 2001, under press.

[17] C. Fillet, J. Marillet, J.L. Dussossoy, J. Phalippou, in: Acers Fall Meeting Proceedings 1997, Cincinatti, in: Ceramic Transactions, Vol. 87, 1998, pp. 531–539.
[18] T. Advocat, C. Fillet, J. Marillet, G. Leturcq, J.M. Boubals, Bonnetier, in: Scientific Basis for Nuclear Waste Management, in: XXI Mater. Res. Soc. Symp. Proc., Vol. 506, 1998.
[19] P. Loiseau, D. Caurant, N. Baffier, L. Mazerolles, C. Fillet, in: Scientific Basis for Nuclear Waste Management, XXIV Mater. Res. Soc. Symp. Proc., Sydney, 2001, under press.
[20] P. Loiseau, D. Caurant, N. Baffier, C. Fillet, in: Scientific Basis for Nuclear Waste Management, XXIV Mater. Res. Soc. Symp. Proc., Sydney, 2001, under press.
[21] T. Advocat, P.J. McGlinn, C Fillet, G. Leturcq, S. Schuller, A. Bonnetier, K. Hart, in: Scientific Basis for Nuclear Waste Management, XXIV Mater. Res. Soc. Symp. Proc., Sydney, 2001, under press.
[22] P.J. Mcglinn, T. Advocat, E. Loi, G. Leturcq, J.P. Mestre, in: Scientific Basis for Nuclear Waste Management, XXIV Mater. Res. Soc. Symp. Proc., Sydney, 2001, under press.
[23] P.J. Mcglinn, K. Hart, E.H. Loi, E.R. Vance, in: Scientific Basis for Nuclear Waste Management, in: XVIII Mater. Res. Soc. Symp. Proc., Vol. 353, 1995, pp. 847–853.
[24] A.E. Ringwood, V.M. Oversby, S.E. Kesson, W. Sinclair, N. Ware, W. Hibberson, A. Major, Nucl. Chem. Waste Management 2 (1981) 287–305.
[25] F. Clinard, Am. Ceram. Bull. 65 (1986) 1181–1187.
[26] G.R. Lumpkin, J. Nucl. Mater. 289 (2001) 136–166.

Discussion

Question de B. Tissot

L'apatite étudiée pour le confinement de l'iode contient beaucoup de plomb. Comment se compare-t-elle, comme matrice de confinement, avec l'iodure de plomb ?

Réponse de C. Guy

Tout d'abord, rappelons que le principe d'élaboration de la céramique de conditionnement de l'iode, $Pb_{10}(VO_4)_{4,8}(PO_4)_{1,2}I_2$ repose sur un frittage réactif sous charge à 700 °C d'un comprimé d'iodure de plomb (PbI_2) entouré d'un orthovanadophosphate de plomb ($Pb_3(VO_4)_{1,6}(PO_4)_{0,4}$) ; ce dernier a une double fonction puisqu'il est un réactif pour la synthèse finale de l'apatite $Pb_{10}(VO_4)_{4,8}(PO_4)_{1,2}I_2$ et qu'il assure le confinement de l'iode pendant la synthèse.

Le conditionnement de l'iode dans une matrice apatitique plutôt que sous une forme d'iodure de plomb est intéressant à plusieurs niveaux.

L'élaboration d'un monolithe diminue considérablement les risques de contamination pendant les phases de conteneurage, de transport et de manutention par rapport à une poudre. Pour mémoire, le centre de stockage de surface de l'Aude destiné aux déchets de Faible Activité n'accepte pas de déchets sous forme de poudres. Le frittage de PbI_2 étant impossible, son enrobage dans une matrice ciment permettrait d'obtenir un monolithe avec, cependant, des inconvénients majeurs liés à une dissolution rapide de l'iode lors du gâchage et à la présence d'eaux interstitielles fortement chargées en iode dans la matrice durcie. Il en résulterait la présence d'une proportion élevée d'iode labile dans un matériau cimentaire ne présentant pas de capacité de rétention de cet élément.

Le frittage à haute température pour élaborer la iodoapatite conduit à un matériau à haute performance en terme de durabilité chimique. Des expériences de dissolution ont été réalisées sur la iodoapatite et sur de l'iodure de plomb. Les vitesses initiales de dissolution sont d'environ 3 ordres de grandeur plus élevés à pH proche de la neutralité pour PbI_2. De plus, la vitesse initiale de dissolution de la iodoapatite diminue au cours du temps ; la mise en solution de l'iode étant vraisemblablement contrôlée par diffusion à travers des couches altérées et/ou des couches néoformées (vanadate de plomb). L'enrobé (orthovanadophosphate) améliore également le confinement en jouant le rôle d'une barrière de confinement avec des propriétés de durabilité chimique équivalentes à celles de la iodoapatite.